Published in final edited form as:
Neurology. 2008 March 4; 70(10): 755–761. doi:10.1212/01.wnl.0000265397.70057.d8.

Cold-Induced Defects of Sodium Channel Gating in Atypical Periodic Paralysis Plus Myotonia

Jadon Webb, B.S. and **Stephen C. Cannon, M.D., Ph.D.**
Department of Neurology and Program in Neuroscience, UT Southwestern Medical Center, Dallas, Texas

Abstract

Background—Missense mutations of the skeletal muscle voltage-gated sodium channel (NaV1.4) are an established cause of several clinically distinct forms of periodic paralysis and myotonia. The mechanistic basis for the phenotypic variability of these allelic disorders of muscle excitability remains unknown. An atypical phenotype with cold-induced hypokalemic paralysis and myotonia at warm temperatures was reported to segregate with the P1158S mutation.

Objective—This study extends the functional characterization of the P1158S mutation and tests the specific hypothesis that impairment of Na channel slow inactivation is a common feature of periodic paralysis.

Methods—Mutant NaV1.4 channels (P1158S) were transiently expressed in HEK cells and characterized by voltage-clamp studies of Na currents.

Results—Wildtype and P1158S channels displayed comparable behavior at 37 °C, but upon cooling to 25 °C mutant channels activated at more negative potentials and slow inactivation was destabilized.

Conclusions—Consistent with other NaV1.4 mutations associated with a paralytic phenotype, the P1158S mutation disrupts slow inactivation. The unique temperature sensitivity of the channel defect may contribute to the unusual clinical phenotype.

Keywords

NaV1.4; channelopathy; skeletal muscle; human

Missense mutations in the voltage-gated sodium channel of skeletal muscle (NaV1.4) have been shown to cause a variety of clinical disorders in which the derangement of muscle excitability is manifest as myotonia or periodic paralysis (1, 2). The spectrum of disorders includes those with myotonia only (potassium aggravated myotonia - PAM), myotonia plus periodic paralysis (paramyotonia congenita - PMC and hyperkalemic periodic paralysis - HyperPP) or only attacks of paralysis (hypokalemic periodic paralysis type 2 – HypoPP-2). The mechanistic basis for the phenotypic variability in this group of allelic disorders of

Correspondence To: Dr. Stephen Cannon, Department of Neurology, UT Southwestern Medical Center, 5323 Harry Hines Boulevard, Dallas, Texas 75390-8813, 214-645-6225, 214-645-6239 (FAX), Steve.cannon@utsouthwestern.edu.

Disclosure: The authors report no conflict of interest

NaV1.4 is not fully established and is of great importance for understanding the regulation of skeletal muscle excitability and for developing improved approaches for the clinical management of these disorders.

The occurrence of atypical clinical presentations provides an opportunity to gain additional insights into these genotype – phenotype associations. An unusual syndrome of myotonia during warm weather for which the predominate feature changed in cold weather to periodic paralysis without myotonia was recently reported (3). The phenotype was inherited as a dominant trait in a large Japanese family with affected members in 5 generations and was associated with a missense mutation in NaV1.4 for which proline 1158 was replaced by serine (P1158S). Unlike the classical presentation of PMC, the myotonia was not aggravated by repeated muscular activity and the paralytic attacks were associated with hypokalemia. Myotonia is not a feature of HypoPP, and when present is considered a basis for excluding this diagnosis (4). The unusual clinical presentation with P1158S is of additional interest in light of the recent discovery that loss-of-function mutations in NaV1.4 may cause HypoPP (5–7); whereas gain-of-function changes are associated with HyperPP, PMC, and PAM (1).

The functional consequences of P1158S were examined in a mammalian expression system and revealed a novel temperature dependent enhancement of channel activation, manifest as a 10 mV leftward (hyperpolarized) shift in the voltage dependence of activation upon cooling from 32 °C to 22 °C (8). Slow inactivation gating, which occurs on a scale of seconds as contrasted with fast inactivation that occurs in msec, was not examined for P1158S in this initial study. Abnormalities in slow inactivation of NaV1.4 have been shown to predispose affected muscle to depolarization-induced attacks of periodic paralysis, but without increased risk for myotonia. Moreover, disrupted slow inactivation is associated with weakness in the HyperPP-PMC complex (9, 10) whereas enhanced slow inactivation is implicated in attacks of weakness for HypoPP type 2 (6). Because the clinical phenotype associated with P1158S has unusual features of both PMC and HypoPP, we have re-examined the functional consequences of P1158S, particularly with regard to slow inactivation. We report a temperature-dependent impairment of slow inactivation induced by cooling and propose that P1158S is therefore mechanistically a variant of PMC-HyperPP rather than HypoPP as previously suggested (3).

Methods

Site-directed mutagenesis

The cDNA for the human skeletal muscle sodium channel (NaV1.4) was provided in the mammalian expression construct pRc/CMV-hSkM1 by Prof. A. L. George, Jr. (11). The P1158S missense mutation was introduced with the QuikChange™ site-directed mutagenesis kit (Stratagene, La Jolla, CA), and was confirmed by sequencing both strands in the regions flanking site 1158.

Sodium channel expression

Transient expression of skeletal muscle sodium channels in human embryonic kidney (HEK) cells and was performed as described previously (12). Briefly, normal WT or mutant sodium

channel NaV1.4 plasmid (0.25 μg/35-mm dish) was cotransfected with the human β_1 accessory subunit (13) at threefold molar excess over NaV1.4, and with a CD8 marker (0.15 μg/35-mm dish) using the calcium phosphate method. After 36 to 72 hours, HEK cells were trypsinized and passaged to 12-mm round glass coverslips for electrophysiological recording. Individual transfection-positive cells were identified by labeling with anti-CD8 antibody cross-linked to microbeads (Dynal, Great Neck, NY) (14).

Whole-cell recording

Na currents were recorded using conventional whole-cell voltage-clamp techniques as described previously (12). Current was measured with an Axopatch 200A amplifier (Axon Instruments, Foster City, CA), filtered at 5 kHz and digitally sampled at 100 kHz using pClamp 9.0 (Axon Instruments). The pipette (internal) solution contained 105 mM CsF, 35 mM NaCl, 10 mM EGTA, and 10 mM Cs-HEPES (pH 7.4). Fluoride was used in the pipette to prolong seal stability. The bath solution contained 140 mM NaCl, 4 mM KCl, 2 mM $CaCl_2$, 1 mM $MgCl_2$, 2.5 mM glucose, and 10 mM Na-HEPES (pH 7.4). Recordings were made in a temperature-controlled chamber that was regulated to either 25°C or 37 °C. Analysis was restricted to cells with maximal peak Na current amplitudes between 0.5 – 15 nA to minimize the effects of endogenous background currents or series resistance artifacts. A stabilization period of 10 minutes was employed after establishing whole-cell access to allow for the leftward (hyperpolarizaed) shift in channel gating that occurs with whole-cell recordings. In addition, the sequence of applying different voltage protocols was kept constant so that characterization of each gating feature was determined at approximately the same time after establishing whole-cell access.

Data analysis

Sodium currents were analyzed with ClampFit 9.0 (Axon Instruments), and parameter estimation for fits of the reduced data was performed with Origin 1.6 (Microcal, Northhampton, MA). The steady-state voltage dependence of activation and inactivation was quantified by fitting the relative peak current to a Boltzmann function with a characteristic midpoint ($V_{1/2}$) and slope factor (k): $I/I_{max} = 1/[1 + \exp((V-V_{1/2})/k)]$. Kinetic data for entry to slow inactivation were fit to a single-exponential decay, whereas adequate fits for recovery required a double-exponential function with two time constants. Symbols with error bars indicate mean ± SEM in all figures.

Results

Although the primary question to be addressed in this study was whether slow inactivation was affected by the P1158S mutation, we also examined activation and fast inactivation to confirm the mutation-dependent changes with cooling as previously reported (8). The expression levels of the wild-type Nav1.4 (WT) and P1158S mutant channels were comparable, as reflected by the mean peak current elicited at −10 mV (3.78 nA ± .71, n = 11 for WT, 4.01 nA ± .85, n = 10 for P1158S). In agreement with the prior expression studies of P1158S (8), we observed a temperature-dependent shift in the voltage the voltage dependence of activation for mutant channels. No difference in activation was detectable at 37 °C (midpoint of the conductance-voltage relation was −39.4 mV ± 1.5, n = 5 for WT; and

−39.0 mV ± 1.8, n = 5 for P1158S). Upon cooling to 25 °C, activation of P1158S mutant channels was shifted −5 mV (hyperpolarized) relative to WT (−26.7 mV ± 1.5, n = 6 for WT compared to −31.9 mV ± 1.9, n = 7 for P1158S, $p = 0.045$; see Supplemental Figure 1). Fast inactivation was not substantially affected by the P1158S mutation. At the provocative temperature of 25 °C, the voltage dependence of fast inactivation was comparable for WT and P1158S channels (midpoint of fast inactivation −73.1 mV ± 1.1, n = 7 for WT and −74.9 mV ± 1.6, n = 9 for P1158S, $p = 0.39$), and we did not detect the −5 mV shift reported previously (8). The rate of fast inactivation was slower for P1158S channels (time constant at strongly depolarized voltages > 40 mV was 0.11 msec ± 0.002 for WT and 0.14 msec ± 0.01 for P1158S). While this 1.3-fold slowing is a robust observation ($p < 0.005$) and comparable to prior observations (8), the functional consequence on muscle fiber excitability is expected to be negligible since impairment in the speed of fast inactivation on the order of 3- to 5-fold is required to create susceptibility to myotonia (15, 16). Overall, our interpretation is in agreement with the initial report on functional properties of P1158S (8) that the most important alteration of fast gating properties for P1158S mutant channels is a hyperpolarized shift of activation at cool temperatures that is absent at 37 °C.

Slow inactivation was studied with paired-pulse voltage protocols. In the first conditioning pulse, a prolonged step of depolarization was applied to induce slow inactivation. The cell was then briefly hyperpolarized (20 ms at −120 mV) to remove fast inactivation, and the extent of slow inactivation was measured as the peak Na current amplitude elicited by a second test pulse, relative to the maximal response recorded in the absence of a conditioning pulse. The entry to slow inactivation was measured as the relative decrement in the peak available Na current (Figure 1A) produced by conditioning the cell at 0 mV for varying durations (from 10 ms to 15 s). At 25 °C, the maximal extent of slow inactivation was reduced for the P1158S mutant, as shown by the higher amplitude of the relative current for the longest conditioning pulse durations (fraction not slow inactivated by 15 sec was 0.19 ± 0.01 for WT and 0.27 ± 0.01 for P1158S, $p < 0.0005$). The kinetics of entry to slow inactivation were quantified by fitting the data with a single exponential to determine the time constant of entry (curves in Figure 1A). The entry time course did not differ between WT (720 ± 47 msec) and P1158S mutants (810 ± 70 msec; $p = 0.38$). At 37 °C the kinetics of slow inactivation were much more rapid as expected (notice the time axis in Figure 1A, left), but again there was no difference the rate of entry for slow inactivation for WT compared to mutant channels. In addition, at 37 °C the difference in the maximal extent of slow inactivation between WT and P1158S channels was reduced.

Recovery from slow inactivation was measured after a conditioning pulse to 0 mV of sufficient duration to induce slow inactivation (30 s at 25 °C or 2 s at 37 °C, each of which is about 20 to 30 times longer than the time constant of entry). The cell was then returned to the recovery potential (−120 mV), and a series of brief test pulses (−10 mV for 3 ms) was applied after recovering for 15, 30, 45… ms and extending to 30 s for experiments at 25 °C (Figure 2B, top). For the studies at 37 °C, the recovery intervals were shorter (1, 2, 3 … 1000 msec), and a single test depolarization was applied after each conditioning pulse. Full recovery was achieved between trials with a repolarization to −120 mV for 3 sec. Recovery was monitored as amplitude of the peak current relative to a control response elicited

without a conditioning step depolarization. Figure 2B (left) shows the recovery data for the P1158S at 25 °C were shifted upward, which was due to the greater fraction of mutant channels resistant to slow inactivation at the end of the conditioning pulse (asymptote for short recovery intervals at the bottom left of the graph: 0.19 ± 0.02, n = 4 for P1185S versus 0.07 ± 0.01, n = 4 for WT; $p = 0.0018$). The time course of slow recovery, however, was indistinguishable between P1158S and WT, and contained two exponential components, Tau_1 = 97 ms (~ 80% of channels that were slow-inactivated) and Tau_2 = 2.8 s (~20%). At 37 °C, all aspects of recovery from slow inactivation were identical for P1158S and WT channels as shown by the superposition of data in Figure 2B (right).

The voltage-dependence of slow inactivation at steady-state was measured by application of long-duration conditioning pulses (2 sec at 37 °C or 15 sec at 25 °C) at voltages ranging from −120 to 0 mV, in 10 mV steps. The durations of these conditioning pulses were sufficiently long to ensure slow inactivation had approached a steady-state value (see Figure 1A), and yet were short enough to maintain cell viability, which did not tolerate longer duration depolarizations at 37 °C. A repolarizing step to −120 mV for 20 ms was applied to enable recovery from fast inactivation, followed by a test pulse to −10 mV to measure the available peak Na current. At 25 °C, the maximal extent of slow inactivation at strongly depolarized potentials was reduced for P1158S (larger remaining relative current in Figure 2 left; WT 0.14 ± 0.01 and P1158S 0.24 ± 0.01; $p < 0.0005$). In addition, the voltage-dependence of slow inactivation was mildly shifted toward more depolarized potentials for the P1158S mutant (half inactivated at −63.2 ± 0.4 mV for WT and −60.5 ± 0.5 mV for P1158S, $p < 0.005$). At 37 °C, however, the voltage dependence of slow inactivation was comparable for WT and P1158S (Figure 2, right), and none of the parameter values were statistically different for the two fitted curves ($p > 0.05$).

Discussion

Mutations of NaV1.4 have been associated with a spectrum of allelic disorders of muscle excitability that span a range of phenotypes including myotonia, periodic paralysis (both hyperkalemic and hypokalemic), and congenital myasthenic syndrome (1). For any given mutation, however, the phenotype is fairly consistent among affected members in a family or even between unrelated families. This genotype – phenotype correlation has led to the notion that specific types of biophysical defects in mutant NaV1.4 channels produce myotonia, for example, whereas other defects lead to paralysis. One of the most consistent associations to emerge from this analysis is that NaV1.4 mutations that disrupt slow inactivation increase the susceptibility to periodic paralysis due to sarcolemmal depolarization and loss of excitability (9, 10, 17). In fact, for every NaV1.4 mutation in which voltage-clamp studies have identified a defect of slow inactivation, periodic paralysis is a prominent feature of the clinical phenotype (Figure 3). The converse is not true; not all mutations associated with periodic paralysis have a recognized defect in slow inactivation. The present study now establishes that P1158S also has impaired slow inactivation. Moreover, a pattern is emerging wherein all of the paralysis-associated mutations that disrupt slow inactivation are at the cytoplasmic end of the 5^{th} or 6^{th} transmembrane segments in domains II or IV, and now III (Figure 3), which are predicted to be the inner vestibule of the ion-conducting pore. The severity of the defect is comparable to that

observed for other NaV1.4 mutations in hyperkalemic periodic paralysis, and has been shown by computer simulation to be sufficient to increase the susceptibility to depolarization-induced loss of excitability (18). A hyperpolarized shift of activation, as observed for P1158S channels, also contributes to the aberrant persistent Na current that depolarizes an affected fiber. These two gain-of-function defects will act synergistically to increase the propensity for attacks of periodic paralysis.

The classification of the clinical phenotype observed in patients with the P1158S mutation was problematic (3). The concurrence of myotonia and periodic paralysis suggested either paramyotonia congenita or hyperkalemic periodic paralysis, and the presence of myotonia would be considered by most experts to be an exclusionary criterion for hypokalemic periodic paralysis (19). However, the venous potassium was low during several spontaneous attacks of weakness and daily K supplementation (16 mEq) alleviated the attacks of weakness. Myotonia was prominent during warm summer months and was reduced in winter during which attacks of paralysis were more common. Paradoxical aggravation of myotonia with repeated effort, i.e. paramyotonia, was not present. The unusual temperature sensitivity of the gating defect in P1158S mutant channels may account for the atypical clinical phenotype. Furthermore, we propose that P1158S should be classified as a variant of the PMC-HyperPP complex because P1158S channels share overlap in the biophysical profile of the gating defects in this group rather than HypoPP. More specifically, the gating defects reported for NaV1.4 in HypoPP Type 2 all share the common feature of loss-of-function changes due to enhanced inactivation (either fast or slow) (5, 6). Conversely, NaV1.4 mutations in the PMC-HyperPP complex all have gain-of-function changes due to either impaired inactivation or enhanced activation. It is tempting to speculate that this dichotomy in gating abnormalities is responsible for the divergent phenotype of serum potassium during an attack of weakness, HypoPP with loss of function and HyperPP with gain of function, but a compelling model to explain the basis for this association has remained unattainable.

P1158S causes gain-of-function changes and we propose the following mechanism for the unusual clinical phenotype. Gating defects are minimal at warm temperatures, and the patients were asymptomatic in a subtropical climate (3). Myotonia occurs at more temperate climates where there is residual enhancement of activation (left shift of voltage dependence) or the small persistent current (8), either of which has been shown by computer simulation to promote myotonic discharges, whereas simulations of disrupted slow inactivation do not. With cooling, the leftward shift of activation becomes more pronounced (Supplementary E-Figure 1) slow inactivation becomes impaired (Figures 1 and 2), and together these defects synergistically increase the risk of a persistent Na current that gives rise to stable depolarization of the resting potential and loss of excitability with paralysis. Mechanistically, the critical feature is the aggravation of the gain-of-function defects by cooling. This scenario is consistent with computer simulations that have demonstrated a transition from normal excitability to myotonia, to periodic paralysis as the severity of Na channel gain-of-function defects is gradually increased (20).

Slow inactivation is cumbersome to study experimentally, which has probably contributed to the paucity of published studies on the temperature sensitivity of this gating process. In this

context, it is notable that the temperature sensitivity for the midpoint in the voltage dependence of slow inactivation is surprisingly much greater than for that of fast inactivation, even for WT channels. For the 12 °C temperature change used in these studies, the midpoint of slow inactivation of WT channels shifted rightward (depolarized) by 15.8 mV upon cooling to 25 °C, whereas fast inactivation shifted by only 2.7 mV. A greater temperature sensitivity for slow inactivation, as compared to fast, has been previously observed (21). In these fast twich IIb fibers from rat omohyoid muscle studied with loose patch recording, however, cooling cause a leftward (hyperpolarized) shift in the voltage dependence of slow inactivation, the opposite direction to our observations. We are unable to explain this discrepancy, other than to suggest it may be related to differences between NaV1.4 behavior in a native muscle environment as contrasted with artificial expression in HEK cells. While the temperature sensitivity for the voltage dependence of slow inactivation may be large in absolute terms, it is the relative difference between WT and P1158S channels at 25 °C that we propose is responsible for producing the increased susceptibility to periodic paralysis.

Supplementary Material

Refer to Web version on PubMed Central for supplementary material.

Acknowledgments

Supported by the NIAMS (RO1-42730) of the National Institutes of Health and the Medical Scientist Training Program (5 T32 GM08014). Kate Miller provided technical assistance.

References

1. Cannon SC. Pathomechanisms in channelopathies of skeletal muscle and brain. Annu Rev Neurosci. 2006; 29:387–415. [PubMed: 16776591]
2. Lehmann-Horn F, Jurkat-Rott K. Voltage-gated ion channels and hereditary disease. Physiol Rev. 1999; 79:1317–1372. [PubMed: 10508236]
3. Sugiura Y, Aoki T, Sugiyama Y, Hida C, Ogata M, Yamamoto T. Temperature-sensitive sodium channelopathy with heat-induced myotonia and cold-induced paralysis. Neurology. 2000; 54:2179–2181. [PubMed: 10851391]
4. Gasser T, Dichgans M, Finsterer J, et al. EFNS Task Force on Molecular Diagnosis of Neurologic Disorders: guidelines for the molecular diagnosis of inherited neurologic diseases. Second of two parts. Eur J Neurol. 2001; 8:407–424. [PubMed: 11554904]
5. Jurkat-Rott K, Mitrovic N, Hang C, et al. Voltage-sensor sodium channel mutations cause hypokalemic periodic paralysis type 2 by enhanced inactivation and reduced current. Proc Natl Acad Sci U S A. 2000; 97:9549–9554. [PubMed: 10944223]
6. Struyk AF, Scoggan KA, Bulman DE, Cannon SC. The human skeletal muscle Na channel mutation R669H associated with hypokalemic periodic paralysis enhances slow inactivation. J Neurosci. 2000; 20:8610–8617. [PubMed: 11102465]
7. Carle T, Lhuillier L, Luce S, et al. Gating defects of a novel Na+ channel mutant causing hypokalemic periodic paralysis. Biochem Biophys Res Commun. 2006; 348:653–661. [PubMed: 16890191]
8. Sugiura Y, Makita N, Li L, et al. Cold induces shifts of voltage dependence in mutant SCN4A, causing hypokalemic periodic paralysis. Neurology. 2003; 61:914–918. [PubMed: 14557559]
9. Cummins TR, Sigworth FJ. Impaired slow inactivation in mutant sodium channels. Biophysical Journal. 1996; 71:227–236. [PubMed: 8804606]

10. Hayward LJ, Sandoval GM, Cannon SC. Defective slow inactivation of sodium channels contributes to familial periodic paralysis. Neurology. 1999; 52:1447–1453. [PubMed: 10227633]
11. Chahine M, Bennett PB, George AL Jr, Horn R. Functional expression and properties of the human skeletal muscle sodium channel. Pflugers Archiv - European Journal of Physiology. 1994; 427:136–142. [PubMed: 8058462]
12. Hayward LJ, Brown RH Jr, Cannon SC. Inactivation defects caused by myotonia-associated mutations in the sodium channel III-IV linker. Journal of General Physiology. 1996; 107:559–576. [PubMed: 8740371]
13. McClatchey AI, Cannon SC, Slaugenhaupt SA, Gusella JF. The cloning and expression of a sodium channel beta 1-subunit cDNA from human brain. Human Molecular Genetics. 1993; 2:745–749. [PubMed: 8394762]
14. Jurman ME, Boland LM, Liu Y, Yellen G. Visual identification of individual transfected cells for electrophysiology using antibody-coated beads. Biotechniques. 1994; 17:874–881.
15. Green D, George A, Cannon S. Human sodium channel gating defects caused by missense mutations in S6 segments associated with myotonia: S804F and V1293I. Journal of Physiology. 1998; 510:685–694. [PubMed: 9660885]
16. Yang N, Ji S, Zhou M, et al. Sodium channel mutations in paramyotonia congenita exhibit similar biophysical phenotypes in vitro. Proceedings of the National Academy of Sciences of the United States of America. 1994; 91:12785–12789. [PubMed: 7809121]
17. Bendahhou S, Cummins TR, Kula RW, Fu YH, Ptacek LJ. Impairment of slow inactivation as a common mechanism for periodic paralysis in DIIS4-S5. Neurology. 2002; 58:1266–1272. [PubMed: 11971097]
18. Hayward LJ, Brown RH Jr, Cannon SC. Slow inactivation differs among mutant Na channels associated with myotonia and periodic paralysis. Biophysical Journal. 1997; 72:1204–1219. [PubMed: 9138567]
19. Lehmann-Horn, F.; Rüdel, R.; Jurkat-Rott, K. Nondystrophic myotonias and periodic paralyses. In: Engel, AG.; Franzini-Armstrong, C., editors. Myology. 3. New York: McGraw-Hill; 2004. p. 1257-1300.
20. Cannon SC, Brown RH Jr, Corey DP. Theoretical reconstruction of myotonia and paralysis caused by incomplete inactivation of sodium channels. Biophysical Journal. 1993; 65:270–288. [PubMed: 8396455]
21. Ruff RL. Effects of temperature on slow and fast inactivation of rat skeletal muscle Na(+) channels. Am J Physiol. 1999; 277:C937–947. [PubMed: 10564086]

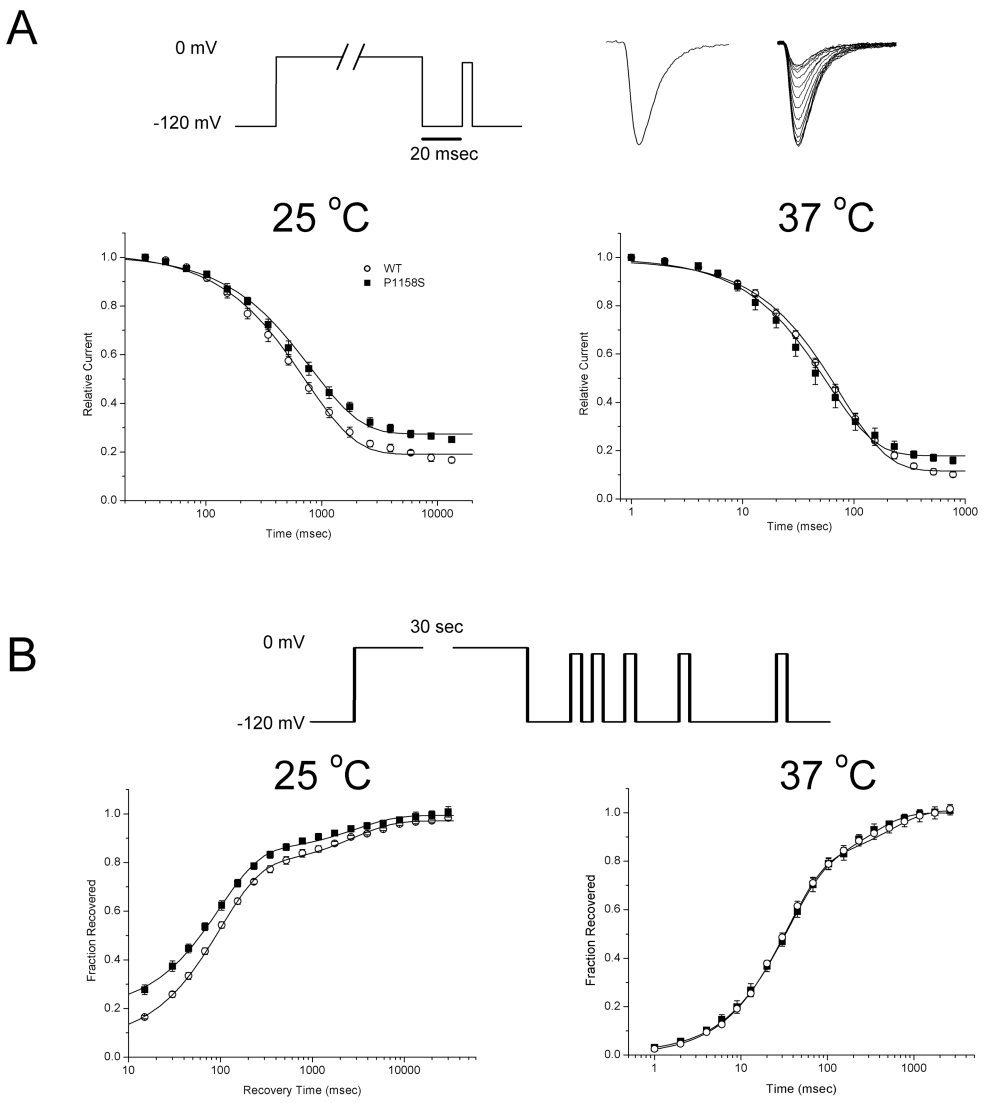

Figure 1.

Kinetics of sodium channel slow inactivation. (A) Entry kinetics of slow inactivation were measured by applying a conditioning pulse to 0 mV of varying duration, followed by a brief hyperpolarization to −120 mV for 20 msec to allow recovery from fast inactivation, and then application of a test depolarization to measure the fractional recovery (pulse protocol, top). Sodium currents (traces at top) show the maximum current elicited in the absence of a conditioning depolarization (left), and a superposition of traces recorded after progressively longer conditioning pulses, which results in smaller peak currents. Plots show the decrement in relative current as slow inactivation ensues with longer duration conditioning pulses (logarithmic scale). Entry to slow inactivation is comparable for P1158S and WT channels at 37 °C, but is less complete for P1158S mutants at 25 °C. (B) Recovery from slow inactivation was monitored by brief test depolarizations after a prolonged conditioning pulse (30 s at 25 °C or 2 sec at 37 °C) to maximally slow inactivate channels (top). At 25 °C, recovery of P1158S channels precedes that of WT, primarily because the extent of slow

inactivation was less complete for P1158S (larger fractional recovery at the shortest recovery times).

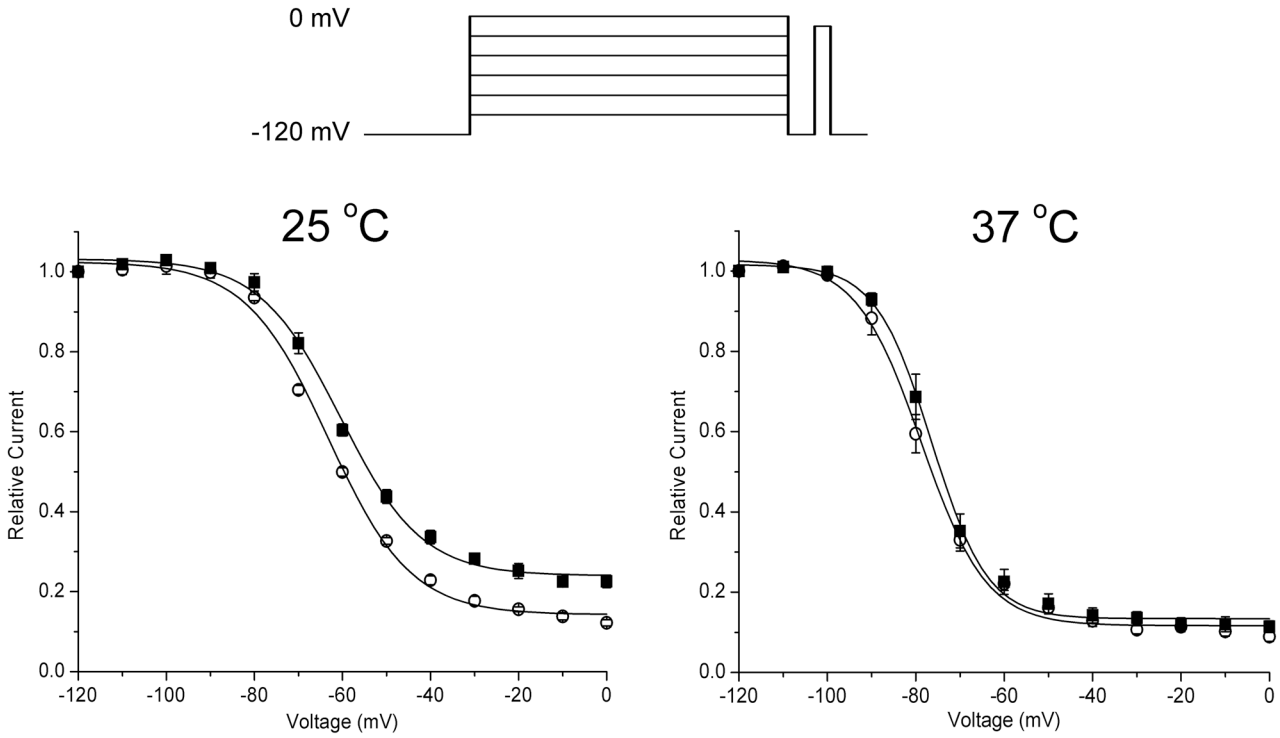

Figure 2.

Voltage dependence of steady-state slow inactivation. Relative available current decreased with progressively more positive conditioning pulses (inset at top) that caused a larger fraction of channels to become slow inactivated. At 25 °C, the voltage dependence of slow inactivation is shifted toward more positive potentials and the extent of slow inactivation at strongly depolarized potentials is reduced (larger available relative current).

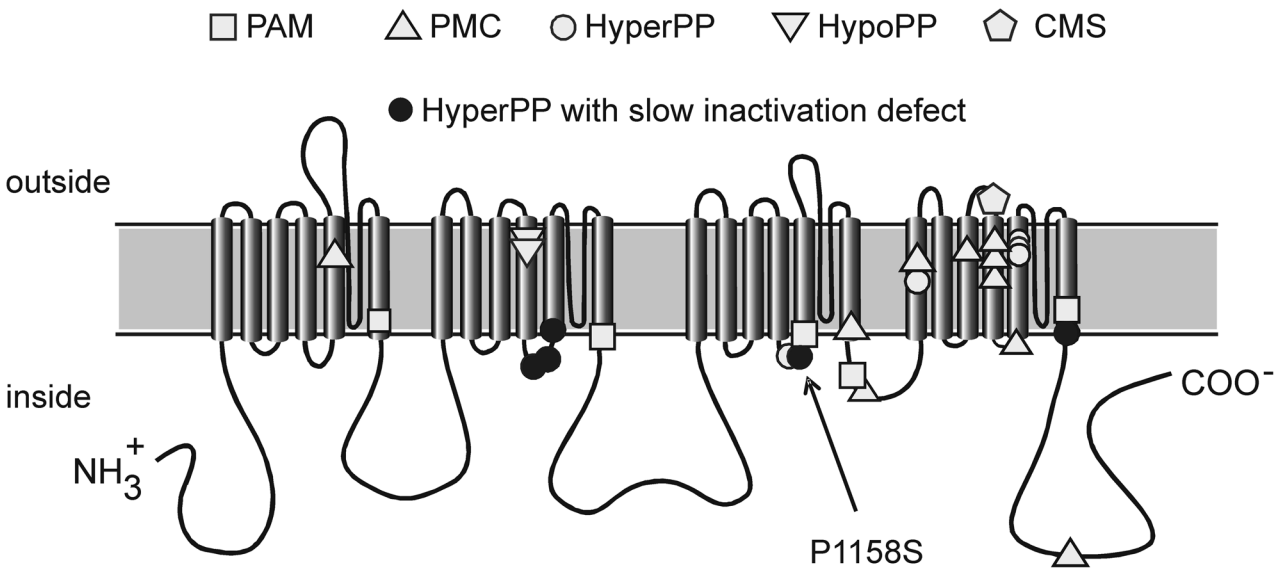

Figure 3.

Membrane-spanning model for NaV1.4 topology and location of missense mutations associated with hyperkalemic periodic paralysis (HyperPP), paramyotonia congenita (PMC), potassium aggravated myotonia (PAM), hypokalemic periodic paralysis type 2 (HypoPP-2), or congenital myasthenic syndrome (CMS). Mutations previously known to disrupt slow inactivation are highlighted and are all associated with HyperPP.